BIOCHEMISTRY
including biophysical chemistry & molecular biology
Article

Biochemistry **2009,** *48,* 8225–8232 8225
DOI: 10.1021/bi901147g

Insights into the Two-Domain Architecture of the Metallocarboxypeptidase Inhibitor from the *Ascaris* Parasite Inferred from the Mechanism of Its Oxidative Folding[†]

Joan L. Arolas, Laura Sanglas, Julia Lorenzo, Sílvia Bronsoms,* and Francesc X. Aviles*

Institut de Biotecnologia i Biomedicina and Departament de Bioquímica i Biologia Molecular, Universitat Autònoma de Barcelona, E-08193 Bellaterra, Barcelona, Spain

Received July 7, 2009; Revised Manuscript Received July 31, 2009

ABSTRACT: The metallocarboxypeptidase inhibitor identified in the intestinal parasite *Ascaris* (ACI) comprises 67 amino acid residues and a novel fold consisting of two structurally similar modules, an N-terminal (NTD) and a C-terminal domain (CTD), each stabilized by two disulfide bonds. Both domains are linked via a connecting segment (CS) that includes a fifth disulfide bond. Here, we investigated the oxidative folding and reductive unfolding of ACI. It folds through a sequential formation of disulfide bonds that finally leads to the accumulation of a heterogeneous population of 5-disulfide non-native scrambled isomers. The reshuffling of these species into the native form constitutes the major kinetic trap of the folding reaction, being efficiently enhanced by the presence of reducing agent or protein disulfide isomerase. The analysis of ACI variants lacking the NTD reveals that this domain is indispensable for the correct folding of such inhibitor, most likely acting as a pro-segment that helps in the acquisition of a CTD native structure, the fundamental inhibitory piece. In addition to the CTD, both the NTD and the CS play a significant role in the function of ACI, as derived from the diminished inhibitory capacity of the truncated ACI variants. Finally, the reductive unfolding and disulfide scrambling analyses reveal that ACI displays an extremely high disulfide and conformational stability, which is consistent with its physiological function in a hostile environment. Altogether, the results provide important clues about the two-domain nature of ACI and may pave the way for its further engineering and development of a minimized inhibitor.

The study of protein folding is still a major challenge in structural and molecular biology. Although working on protein folding is usually difficult due to the transient nature of folding intermediates, the particular chemistry of disulfide-bond formation allows circumventing this problem thanks to the trapping of disulfide-bonded intermediates by alkylation or acidification (*1*, *2*). A deeper understanding on the nature of these folding intermediates would provide the possibility to conceive approaches to deal with diseases caused by protein misfolding and also help to improve the recovery of recombinant proteins for biotechnological applications (*3*−*5*). Extensive investigation on model proteins such as bovine pancreatic trypsin inhibitor (BPTI[1]), ribonuclease A, lyzozyme, and hirudin (*6*−*9*), among others (*10*−*13*), has set up the basis for studies of oxidative folding, that is, the composite process by which a reduced and unfolded protein acquires both its native disulfide bonds and its native structure. The disulfide folding pathway is elucidated from the order of formation of disulfide bonds, and characterized by the heterogeneity and disulfide pairings (native or non-native) of the intermediates that arise during the oxidative folding reaction (*14*). A great diversity of folding mechanisms is observed among the numerous proteins that have been studied to date using this technique (*15*, *16*). At the two extremes of this diversity we find BPTI and hirudin, two well-known serine protease inhibitors. The former protein folds via a limited number of intermediates containing native disulfide bonds and native-like structures (*17*), while the folding of the later proceeds through a highly heterogeneous population of intermediates with the presence of fully oxidized non-native (scrambled) isomers (*18*).

A new metallocarboxypeptidase (MCP) inhibitor has been recently isolated from *Ascaris*, the most common human parasite of the gastrointestinal tract that causes the pandemic disease ascariasis (*19*). The inhibitor, termed ACI, is 67-residues long and does not show significant sequence homology with any known protein. Recombinant ACI is fully functional and displays nanomolar inhibition constants against digestive and mast-cell A/B-type MCPs, which is in good agreement with its localization within the *Ascaris* roundworm, i.e. in body wall, intestine, female reproductive tract, and fertilized eggs. The crystal structure of ACI in complex with human carboxypeptidase A1 (hCPA1), one of its potential targets *in vivo*, shows a protein with a novel fold consisting of two structurally similar tandem modules (Figure 1A,B), an N-terminal (NTD) and a C-terminal domain (CTD), which are linked by a connecting segment (CS). Each

[†]This study was supported by Grants BIO2007-68046 (Spanish Ministry of Science and Innovation) and SGR01037 (National Catalan Government). L.S. is beneficiary of a predoctoral fellowship from the Spanish Ministry of Science and Innovation.

*To whom correspondence should be addressed. S.B.: tel, +34-93-581-1231; fax, +34-93-581-2011; e-mail, silvia.bronsoms@uab.cat. F.X.A.: tel, +34-93-581-1315; fax, +34-93-581-2011; e-mail, francescxavier.aviles@uab.es.

[1]Abbreviations: A/L/T/CI, *Ascaris*/leech/tick carboxypeptidase inhibitor; BPTI, bovine pancreatic trypsin inhibitor; CS, connecting segment; CTD, C-terminal domain; DTT, dithiothreitol; GdnHCl, guanidine hydrochloride; GdnSCN, guanidine thiocyanate; GSH, reduced glutathione; GSSG, oxidized glutathione; K_i, inhibition constant; MALDI-TOF MS, matrix-assisted laser desorption/ionization time-of-flight mass spectrometry; (M)CP, (metallo)carboxypeptidase; N, native protein; NTD, N-terminal domain; PDI, protein disulfide isomerase; R, reduced/unfolded protein; RP-HPLC, reversed-phase high performance liquid chromatography; RT, room temperature; TCEP, tris(2-carboxyethyl)phosphine; TFA, trifluoroacetic acid.

Published on Web 07/31/2009

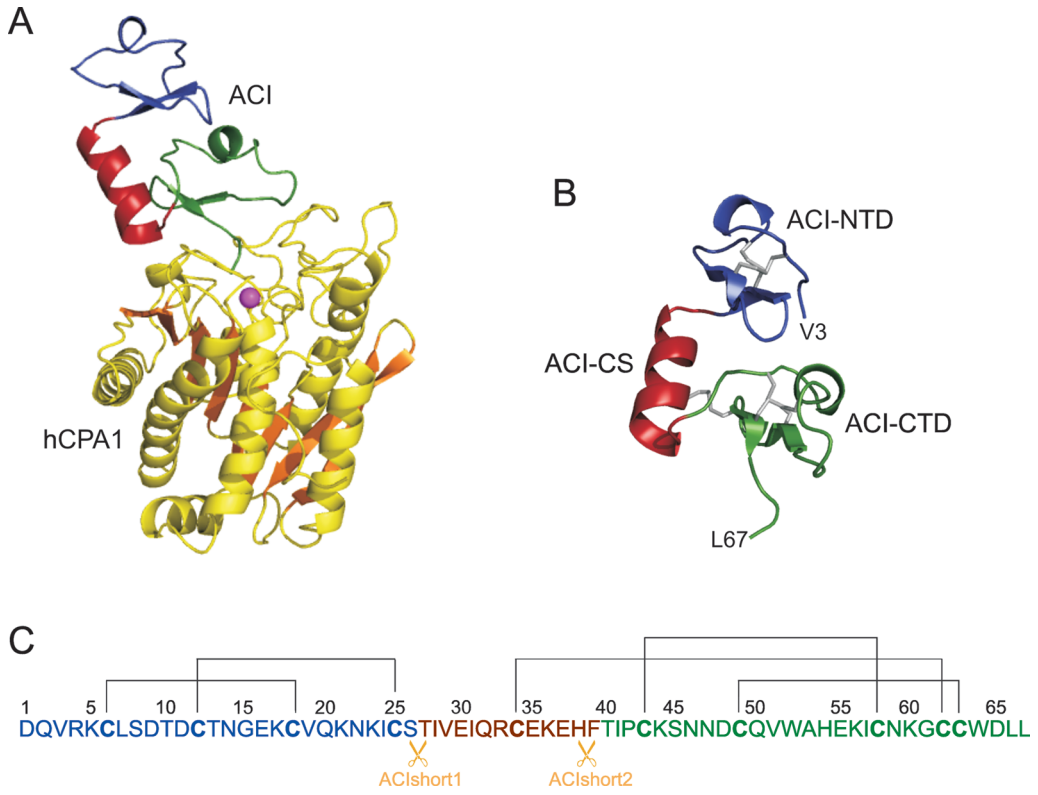

FIGURE 1: Structure of ACI and its complex with hCPA1. (A) Richardson plot of the complex of ACI (NTD in blue, CS in red, and CTD in green) and hCPA1 (α-helices and turns in yellow, β-strands in orange, catalytic zinc ion as a magenta sphere) (PDB code 3FJU). Figure prepared with PyMOL. (B) Richardson plot of ACI taken from (A), showing its domain architecture and regular secondary structure elements (ribbons for the concatenated 1,4-turns and the α-helix, arrows for β-strands). The five native disulfide bonds (Cys^{6}−Cys^{18}; Cys^{12}−Cys^{25}; Cys^{34}−Cys^{62}; Cys^{43}−Cys^{58}; and Cys^{49}−Cys^{63}) are shown as gray sticks. The N- and C-terminal residues are labeled. (C) Amino acid sequence of ACI. The native disulfide-bond pairings are schematically shown above the sequence. The limits for the ACIshort1 and ACIshort2 constructs are indicated below the sequence.

domain comprises a small helix and a C-terminal β-sheet that are stabilized by two disulfide bonds (see Figure 1C). The CS includes an α-helix, which is linked to the β-sheet of the CTD by an external disulfide bond. Binding and inhibition of hCPA1 is exerted by the C-terminal tail of ACI, which enters the funnel-like active-site cavity of the carboxypeptidase and approaches the catalytic zinc ion. Secondary contacts come from the tip and the center of the N-terminal β-strand of the CTD, as well as the end of the CS, contributing to the formation of a more stable complex. Therefore, the NTD of ACI is not involved directly in the interaction with hCPA1. Preliminary conformational studies by CD and NMR spectroscopy indicate that ACI is highly stable and only denatures by the simultaneous presence of both denaturing and reducing agents (*19*).

The main aims of this study are to characterize the oxidative folding and reductive unfolding pathways of ACI and also to determine the role of each part of the molecule in its folding and activity. To clarify the latter issue we have constructed two truncated variants of ACI lacking the NTD or both the NTD and CS and have characterized their folding pathway and inhibitory capability.

MATERIALS AND METHODS

Protein Expression and Purification. Recombinant ACI was obtained by heterologous overexpression in *Escherichia coli* as previously published (*19*). Briefly, ACI was cloned into the pET-32a vector and transformed in *E. coli* Origami2 (DE3) cells. Expression of the protein was performed in Luria−Bertani medium inducing with 0.5 mM isopropyl-β-D-thiogalactopyranoside at 18 °C. The thioredoxin-hexahistidine-ACI fusion protein was purified by Ni^{2+}-affinity chromatography (HiTrap HP column, GE Healthcare) and subsequently digested with tobacco-etch-virus protease, which leaves a glycine residue at the N-terminus of the protein. The inhibitor was finally purified to homogeneity by reversed-phase high performance liquid chromatography (RP-HPLC) in a Waters Alliance apparatus and stored lyophilized. The ACI variants lacking the NTD (ACIshort1; Thr^{27}−Leu^{67}) and the NTD plus the CS (ACIshort2; Phe^{39}−Leu^{67}, with Cys^{62} replaced by a serine residue) were generated by PCR using the pET-32a-ACI vector as template. Both ACI variants were expressed and purified as described for the wild type (WT) form. Protein identity and purity were confirmed by mass spectrometry (MS), automated Edman degradation and SDS−PAGE.

Oxidative Folding. Native protein (2 mg) was incubated in 0.1 M Tris-HCl, pH 8.5, containing 6 M guanidine thiocyanate (GdnSCN) and 100 mM dithiothreitol (DTT) for at least 2 h at room temperature (RT). The chemical reagents were purchased from Sigma unless otherwise stated. To initiate folding, the reduced and unfolded protein was passed through a PD-10 column (Sephadex G-25; GE Healthcare), previously equilibrated with 0.1 M Tris-HCl, pH 7.2 or 8.5. After elution in a volume of 1.2 mL, the protein was immediately diluted to a final concentration of 0.5 mg/mL in the same buffer, both in the absence (Control −) and presence of redox agents: 0.25 mM 2-mercaptoethanol (Control +), 0.5 mM oxidized glutathione (GSSG), or 0.5 mM/1 mM oxidized/reduced glutathione (GSSG/GSH). In some cases selected concentrations of NaCl (0.2 M), protein disulfide isomerase (PDI) (2 μM), or denaturant

(0.5−4 M guanidine hydrochloride; GdnHCl) were added to the reaction. To monitor folding, aliquots were removed at various time intervals and quenched with 4% aqueous trifluoroacetic acid (TFA). Acid-trapped intermediates were subsequently analyzed by RP-HPLC in a 4.6-mm Jupiter C4 column (Phenomenex) using a linear gradient from 25 to 35% (for WT ACI) or 23−33% (for ACIshort1 and ACIshort2) acetonitrile with 0.1% TFA at a flow rate of 0.75 mL/min for 50 min.

Reductive Unfolding. Native protein (0.5 mg/mL) was dissolved at RT in either 0.1 M Tris-HCl, pH 8.5, or 0.1 M sodium acetate, pH 4.5, containing increasing concentrations (1−400 mM) of DTT or tris(2-carboxyethyl)phosphine (TCEP), respectively. To monitor the unfolding reaction, time-course aliquots of the samples were trapped with 4% aqueous TFA and analyzed by RP-HPLC as detailed in Oxidative Folding.

Disulfide Scrambling. Native protein was dissolved to a final concentration of 0.5 mg/mL in 0.1 M Tris-HCl, pH 8.5, containing 0.25 mM 2-mercaptoethanol as thiol initiator and different concentrations of denaturants (0−8 M urea, 0−8 M GdnHCl, or 0−6 M GdnSCN). The reaction of disulfide scrambling was allowed to reach equilibrium typically for 20 h at RT. The samples were then quenched with 4% aqueous TFA and analyzed by RP-HPLC as detailed in Oxidative Folding.

Disulfide Pairing Analysis. To determine the number of disulfide bonds, acid-trapped intermediates that populate the oxidative folding and reductive unfolding of ACI were purified by RP-HPLC using the conditions described in Oxidative Folding and lyophilized. Each sample was alkylated with 0.1 M Tris-HCl, pH 8.5, containing 0.1 M 4-vinylpyridine for 45 min at RT in the dark. The derivatized protein was then freed from reagents by RP-HPLC, and analyzed by matrix-assisted laser desorption/ionization time-of-flight (MALDI-TOF) MS (+105 Da for each free cysteine). Samples were mixed with a matrix solution (1:1, v/v) of 10 mg/mL 2,6-dihydroxyacetophenone (Sigma) dissolved in 30% acetonitrile containing 20 mM dibasic ammonium citrate, pH 5.5. 0.5 μL of the mixture was spotted onto the MALDI-TOF plate using the dried-droplet method. Mass spectra were acquired in an Ultraflex mass spectrometer (Bruker) equipped with a 337 nm laser in linear mode geometry under 20 kV and ~300 laser shots. A mixture of proteins from Bruker (Protein calibration standard I; mass range 3,000−25,000 Da) was used as a calibration standard. To determine the disulfide pairings, purified and lyophilized acid-trapped intermediates were digested with endoproteinase Lys-C (Roche Applied Science) in 20 mM Tris-HCl buffer, pH 8.0, for 4 h at 37 °C using an enzyme:substrate ratio of 1:40 (w/w), and further analyzed by MALDI-TOF MS. The obtained peptide mass fingerprint was compared with the expected proteolytic digest of ACI using the program SequenceEditor (Bruker). The N-terminal amino acid sequence of selected species was determined by automated Edman degradation in an Applied Biosystems model Procise 492 protein sequencer.

CPA Inhibitory Experiments. The inhibitory activity of different ACI forms was tested by measuring the inhibition of hydrolysis of the chromogenic substrate *N*-(4-methoxyphenylazoformyl)-Phe-OH (Bachem) by human CPA1 at 350 nm using a Cary 400 UV−vis spectrophotometer (Varian). The assays were performed in 50 mM Tris-HCl, 100 mM NaCl, pH 7.5, at a substrate concentration of 100 μM. Inhibition constants (K_is) against human CPA1 were determined using pre-steady-state kinetics as reported for tight-binding inhibitors (*20*). The concentration of ACI variants in solution was determined by measuring the absorbance at 280 nm and using the calculated absorption coefficients $E_{0.1\%} = 1.49$, 2.32, and 3.30, for WT ACI, ACIshort1, and ACIshort2, respectively.

RESULTS

Oxidative Folding of ACI. The oxidative folding of ACI was examined by acid-trapping and RP-HPLC analysis of the disulfide intermediates that accumulate along the folding process. The reduced and unfolded protein (R) was allowed to refold in Tris-HCl, pH 7.2 or 8.5, in the absence and presence of different redox agents (for details, see Materials and Methods). Similar RP-HPLC profiles were observed up to 8 h of folding reaction, at both pH 7.2 and 8.5, regardless of the absence (Control −) and presence (Control +) of 2-mercaptoethanol (Figure 2A,B). However, the presence of reducing agent in the reaction mixture substantially affected the last stages of folding by decreasing the accumulation of intermediates and favoring the attainment of the native structure (N). The analysis by MS of the acid-trapped

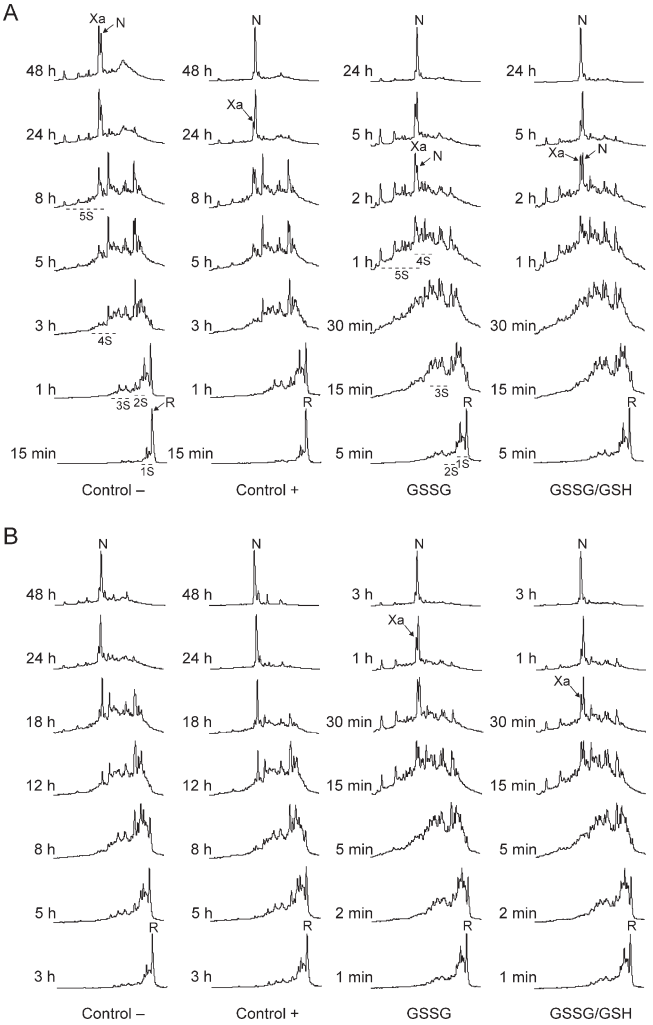

FIGURE 2: Oxidative folding of ACI. RP-HPLC traces of the acid-trapped intermediates that accumulate along the oxidative folding of ACI. The reactions were performed in Tris-HCl, pH 7.2 (A) or 8.5 (B), in the absence (Control −) and presence (Control +) of 0.25 mM 2-mercaptoethanol, 0.5 mM GSSG, or a mixture of GSSG and GSH (0.5 mM and 1 mM) as detailed under Materials and Methods. The retention times of the native (N) and fully reduced/unfolded (R) forms are labeled. XS represents an ensemble of species with X number of disulfide bonds as determined by alkylation with 4-vinylpyridine and subsequent analysis by MALDI-TOF MS. Xa stands for a major 5-disulfide scrambled isomer.

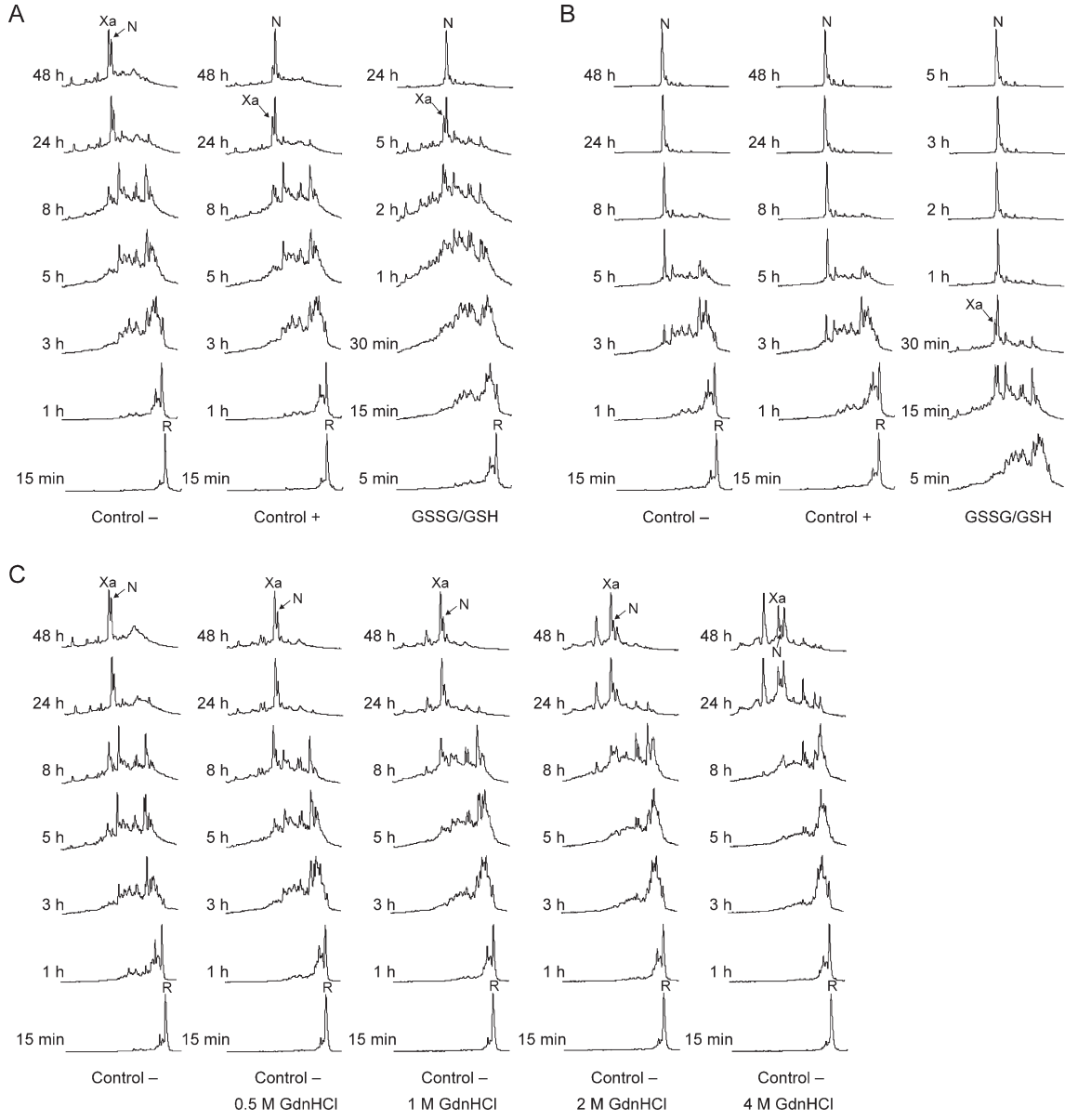

FIGURE 3: Oxidative folding of ACI at physiological and denaturing conditions. RP-HPLC traces of the acid-trapped intermediates that occur along the oxidative folding of ACI carried out in Tris-HCl, pH 7.2, in the absence (Control −) and presence (Control +) of 0.25 mM 2-mercaptoethanol, or 0.5 mM/1 mM GSSG/GSH. 0.2 M NaCl (A), 0.2 M NaCl plus 2 μM PDI (B), or 0.5−4 M GdnHCl (C) was added to the folding reaction. The retention times of the native (N) and fully reduced/unfolded (R) forms are labeled. Xa stands for a major 5-disulfide scrambled isomer.

intermediates further derivatized with vinylpyridine showed a sequential formation (packing) of 1-, 2-, 3-, 4-, and 5-disulfide species. The strongest kinetic trap of the folding reaction appeared to be the reshuffling (consolidation) of 5-disulfide scrambled isomers into native ACI, which is promoted by the presence of reducing agent (2-mercaptoethanol or GSH). Unfortunately, the major scrambled isomer (Xa) could not be analyzed in terms of function and disulfide pairings due to its close proximity in elution with N. As expected, the addition of oxidizing agent (GSSG) enhanced the formation of intermediates at the early steps of folding, leading to an improved folding process. Also, the use of a buffer with pH 8.5, which coincides with the pK_a of the cysteine side chain, significantly affected the overall folding rate, slowing down the first steps of folding and accelerating the final consolidation of scrambled isomers into native protein (see Control − in Figure 2A vs 2B).

To mimic the conditions inside the cell, the oxidative folding of ACI was studied at pH 7.2 in the presence of NaCl and of the protein folding catalyst PDI (Figure 3A,B). The addition of a physiological concentration of NaCl did not significantly affect the folding of ACI, indicating the absence of competing ionic interactions and/or electrostatic repulsions during the folding process. However, the addition of PDI dramatically accelerated the folding rate, leading to completion of the reaction after 8 h in the absence of GSSG and 1 h in its presence. The same behavior was observed when folding was performed at pH 8.5, confirming that the acceleration of the folding rate was due to a faster disulfide exchange that avoids the accumulation of scrambled isomers, which were rapidly funneled to N by the action of PDI. ACI was also refolded at pH 7.2 in the presence of selected concentrations of denaturant (Figure 3C) to study the role of noncovalent contacts on its oxidative folding. Increasing concentrations of GdnHCl correlated with a higher accumulation of

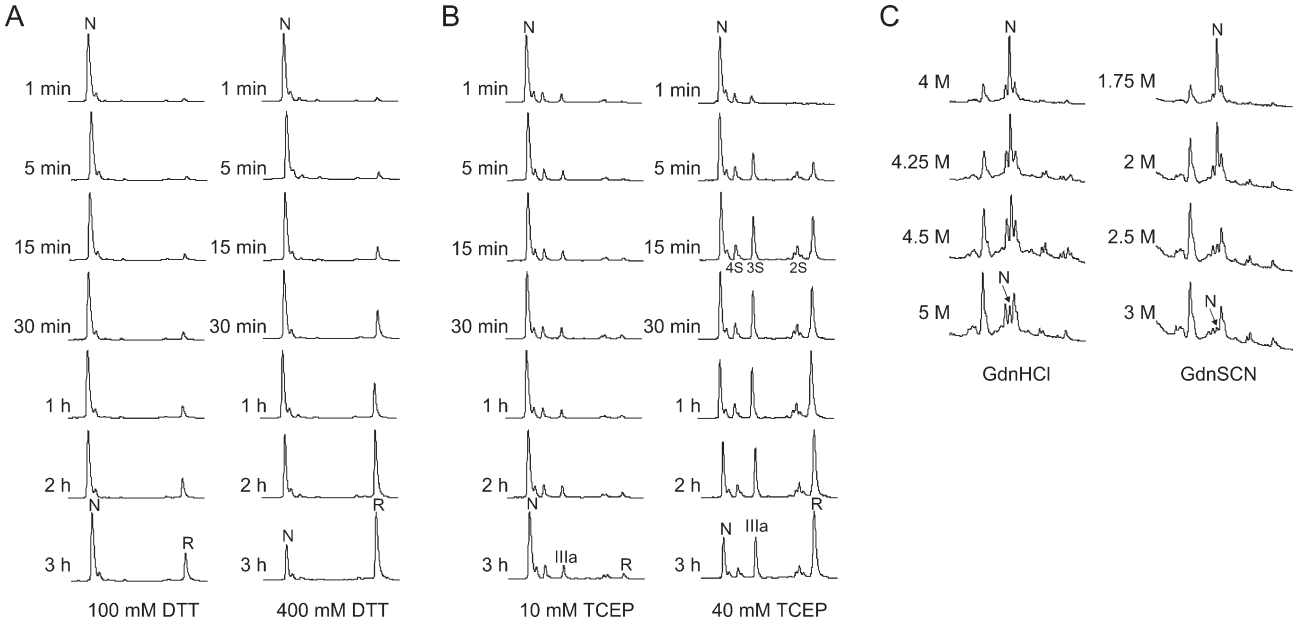

FIGURE 4: Reductive unfolding and disulfide scrambling of ACI. RP-HPLC traces of the acid-trapped intermediates generated by reductive unfolding or disulfide scrambling. Native ACI was reduced with increasing concentrations of DTT in Tris-HCl, pH 8.5 (A), or TCEP in sodium acetate, pH 4.5 (B). N and R indicate the native and fully reduced/unfolded forms, respectively. 2S, 3S and 4S represent ensembles of species with the corresponding number of disulfide bonds. IIIa stands for a major 3-disulfide intermediate. (C) Native ACI was denatured by incubation for 20 h in Tris-HCl, pH 8.5, containing 0.25 mM 2-mercaptoethanol as thiol initiator and the indicated concentration of denaturant.

scrambled isomers at the end of the folding reaction, and therefore, in lower amounts of native protein. Thus, unlike for other small disulfide-rich proteins like leech carboxypeptidase inhibitor (LCI) (*21*), in ACI the addition of small denaturant concentrations did not promote the acquisition of N.

Reductive Unfolding of ACI. The reductive unfolding of ACI was investigated by acid-trapping and RP-HPLC analysis of the disulfide intermediates that accumulate along the unfolding process. The native protein was reduced in either Tris-HCl, pH 8.5, using DTT or sodium acetate, pH 4.5, using TCEP (Figure 4A,B). High concentrations of DTT (i.e., 100 mM) were necessary to reduce native ACI. The unfolding reaction followed an apparent all-or-none mechanism (*22*), with the concerted reduction of the five disulfide bonds that resulted in the accumulation of minute amounts of intermediates. The use of TCEP as reducing agent strongly altered the unfolding reaction, giving rise to the noticeable accumulation of three fractions in the RP-HPLC chromatogram. The intermediates contained in these fractions were derivatized with vinylpyridine and further analyzed by MS. The analysis revealed the successive accumulation of 4-, 3-, and 2-disulfide species before reaching the fully reduced/unfolded form. The analysis by automated Edman degradation of the single intermediate found inside 3S (termed IIIa) revealed the presence of pyridylethyl groups at positions Cys^6, Cys^{12}, Cys^{18}, and Cys^{25} (data not shown). Therefore, IIIa contains four free cysteines instead of two disulfide bonds in the NTD. Importantly, despite the lack of two disulfide bonds this unfolding intermediate shows a very similar affinity toward hCPA1 as compared to the native form, suggested by a nearly indistinguishable K_i determined for both forms against this enzyme (Table 1). Alkylation and subsequent Edman analysis of the 4S fraction showed the presence of two 4-disulfide intermediates lacking either the Cys^6−Cys^{18} or the Cys^{12}−Cys^{25} disulfide bond. The disulfide pairings of 2S could not be determined owing to the presence of a complex mixture of 2-disulfide intermediates inside this fraction.

Table 1: Inhibition Constants (K_i) of ACI Variants and Intermediates against hCPA1[a]

	K_i (nM)
N ACI	1.6 ± 0.2
IIIa ACI	1.9 ± 0.3
N ACIshort1	39.8 ± 3.7
Xa ACIshort1	205.5 ± 5.2
N ACIshort2	2400 ± 100
Xa ACIshort2	2600 ± 400

[a]The values are given as mean ± SD.

Disulfide Scrambling of ACI. It is known that in the presence of a thiol initiator and denaturant, unfolding of a native disulfide-containing protein results in reshuffling of its native disulfide bonds, a process called disulfide scrambling (*23*). Unfolding of native ACI was performed at pH 8.5 in the presence of 2-mercaptoethanol and increasing concentrations of different denaturants (urea, GdnHCl and GdnSCN). After reaching equilibrium the reactions were analyzed by RP-HPLC (Figure 4C). The use of high concentrations of GdnHCl and of GdnSCN promoted the reshuffling of native ACI into scrambled isomers, which reflects the degree of unfolding of native ACI. The exact percentages of scrambled isomers and N could not be integrated due to the overlap in their RP-HPLC elution times; the midpoint denaturant concentrations were about 4.25 M GdnHCl and 1.9 M GdnSCN. No fraction of scrambled isomers was detected by incubation with 0−8 M urea (data not shown).

Oxidative Folding of ACIshort1 and ACIshort2. ACIshort1 lacks the NTD and therefore displays three disulfide bonds (two in the CTD plus one linking the CS and the CTD). ACIshort2 lacks both the NTD and the CS, which implies the loss of a third disulfide bond, i.e. it only comprises the two disulfide bonds of the CTD. The oxidative folding of both truncated variants was examined by acid-trapping and RP-HPLC analysis

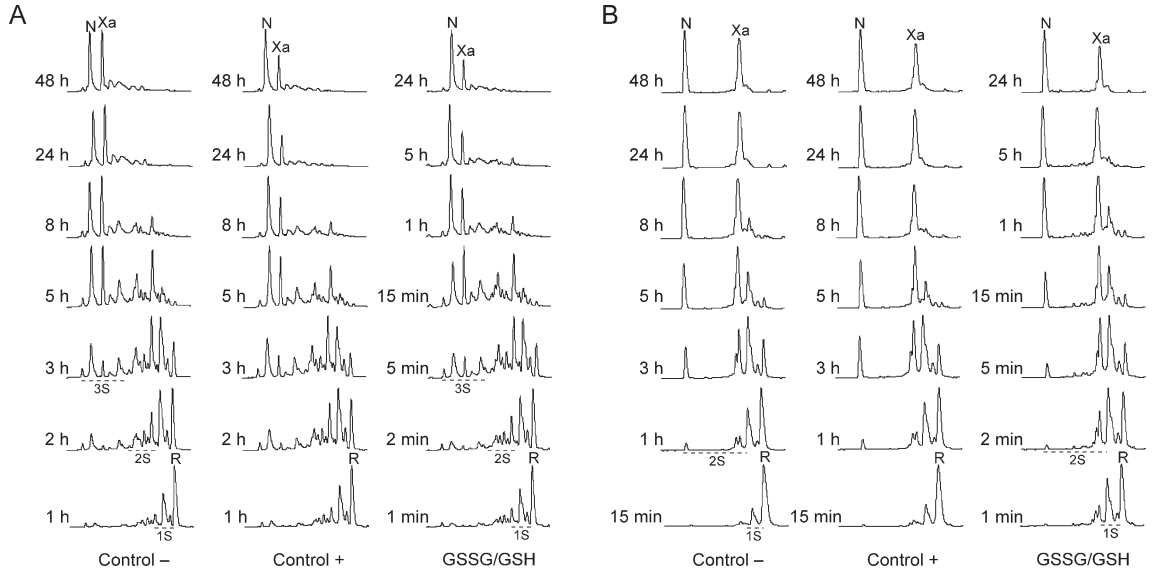

FIGURE 5: Oxidative folding of truncated ACI variants. RP-HPLC traces of the acid-trapped intermediates that accumulate along the oxidative folding of ACIshort1 (A) and ACIshort2 (B). The reactions were performed in Tris-HCl, pH 8.5, in the absence (Control −) and presence (Control +) of 0.25 mM 2-mercaptoethanol or a mixture of GSSG and GSH (0.5 mM and 1 mM). The retention times of the native (N) and fully reduced/unfolded (R) forms are labeled. *X*S represents an ensemble of species with *X* number of disulfide bonds. Xa stands for a major 3- (ACIshort1) and 2-disulfide (ACIshort2) scrambled isomer.

of the disulfide intermediates that accumulate along the folding process. The reduced and unfolded proteins were allowed to refold in Tris-HCl, pH 8.5, in the absence and presence of different redox agents (Figure 5A,B). For ACIshort1 similar RP-HPLC profiles were observed up to 5 h regardless of the absence (Control −) and presence (Control +) of 2-mercaptoethanol. The addition of GSSG strongly accelerated the formation of intermediates at the beginning of the folding process (data not shown). The analysis by MS of the acid-trapped intermediates further derivatized with vinylpyridine showed a sequential formation of 1-, 2-, and 3-disulfide species. The presence of reducing agent in the reaction mixture significantly affected the last stages of folding by enhancing the conversion of a Xa-like isomer into N. This major 3-disulfide scrambled isomer displays a low inhibitory capability (Table 1). The native form of ACIshort1 also shows a higher inhibition constant compared to WT ACI (~25-fold increase). However, this form comprises the three native disulfide bonds of the CTD and CS of ACI, that is, Cys^{34}−Cys^{62}, Cys^{43}−Cys^{58}, and Cys^{49}−Cys^{63}, as indicated by digestion with Lys-C and further MS analysis: Peptides of 1451.73 and 3515.62 Da, corresponding to residues ^{37}EHF-TIP$\underline{C}$K^{44}+^{57}IC$\underline{N}$K^{60} and (G)TIVEIQR$\underline{C}$EK^{36}+^{45}SNND$\underline{C}$ QV-WA$\underline{H}$EK^{56}+^{6T}G$\underline{C}\underline{C}$ WDLL^{67}, respectively. The numbering is based on the WT ACI sequence.

For ACIshort2 there was a rapid formation of a few 1- and 2-disulfide intermediates that was strongly sped up by the addition of GSSG (data not shown). Again the presence of reducing agent in the reaction mixture significantly affected the last stages of folding by promoting the conversion of an Xa-like isomer into N. Xa ACIshort2 is a major 2-disulfide scrambled isomer with a very low inhibitory potential (Table 1). Noteworthy, the native form of ACIshort2 also shows a very low inhibitory activity, despite the fact that it comprises the two native disulfide bonds of the CTD: Cys^{43}−Cys^{58}, and Cys^{49}−Cys^{63}. This is indicated by digestion with Lys-C and further MS analysis: Peptides of 1240.74 and 2222.95 Da, corresponding to residues (G)FTIP-$\underline{C}$K^{44}+^{57}I$\underline{C}$NK^{60} and ^{45}SNND$\underline{C}$ QVWAHEK^{56}+^{61}GS$\underline{C}$W-DLL^{67}, respectively. The numbering is based on the WT ACI sequence. In summary, unlike WT ACI, the folding of both ACIshort1 and ACIshort2 cannot reach completion since at the end of the reaction only 40−50% and 60−70% of the protein was recovered as native form in the absence and presence of thiol catalyst, respectively (see Figure 5A,B).

DISCUSSION

ACI is the only metallocarboxypeptidase inhibitor found at the defense barrier of *Ascaris*, which mainly consists of a battery of selective protease inhibitors that protects the parasite from host enzymes and the immune system (*19*). In this work, we have comprehensively analyzed the pathways of oxidative folding and reductive unfolding of ACI. It folds through the sequential formation of 1-, 2-, 3-, and 4-disulfide intermediates that subsequently evolve into a mixture of 5-disulfide scrambled isomers. Among them the Xa scrambled isomer accumulates to a major extent, eluting very close to native ACI in the reversed-phase chromatogram. This scrambled species could arise from the presence of two consecutive cysteines located at the C-terminus of ACI (Cys^{62} and Cys^{63}), which could easily lead to divergent disulfide pairings. A similar phenomenon is observed in the oxidative folding of tick carboxypeptidase inhibitor (TCI) (*24*). At neutral pH Xa accumulates to similar percentages as N after 48 h of reaction (Control −), thus acting as an important kinetic trap of the ACI folding process. Only the presence of reducing agent or PDI efficiently promotes its reshuffling into N. The highly efficient folding obtained in the presence of PDI demonstrates the important role that this enzyme may have on ACI folding *in vivo*. The effect of these catalysts is clearly exerted over the kinetic traps, i.e. the scrambled population, promoting their rapid consolidation into native protein and avoiding the accumulation of the metastable intermediate Xa. This strong effect on the formation of native protein from kinetic traps has also been described for BPTI and hirudin (*25*, *26*).

The folding of ACIshort1 and ACIshort2, both lacking the NTD, cannot reach a unique predominant form, which implies that the absence of this domain has influence on the folding of the CTD. Therefore, the two domains of ACI do not fold

independently, unlike the case of TCI, which consists of two tandem structurally similar modules linked by a short and flexible linker (*27*). In TCI each domain, comprising three disulfide bonds, folds and unfolds autonomously without establishing interdomain disulfide bonds (*24*, *28*). Also, there are no contacts between both domains. The N-terminal domain of TCI is directly involved in the binding of MCPs, interacting with an exosite of the enzyme surface which contributes to high inhibitory capability (*29*). We have previously hypothesized that the NTD of ACI could target digestive enzymes different from MCPs present in the host gut (*19*). Apart from this potential function, we observe here that, after the addition of optimal concentrations of thiol catalysts and 48 h of oxidative folding, less than 70% of ACIshort1 or ACIshort2 variants are recovered as native form. These results demonstrate that the NTD is essential for the correct folding of ACI, since neither the CTD nor the CTD plus the CS can fold efficiently, which provides a plausible explanation for the two-domain architecture of this molecule. The NTD would guide the folding of the CTD most likely through transient interdomain disulfide interactions, acting as an intramolecular chaperone. There are many examples of pro-segments required for correct folding of their associated proteins, but only a few of them correspond to small disulfide-rich proteins (*30*). In the case of guanylyl cyclase activating peptide, the pro-region contributes to both the correct disulfide-coupled folding of the mature protein and the dimerization of the molecule (*31*). In the case of ACI, the NTD facilitates the disulfide reshuffling of the protein but is not removed after protein folding, as in the case of pro-segments, maybe owing to its contribution to ACI function.

Indeed, it is surprising to note the important role of the NTD for the function of ACI as inhibitor of MCPs, particularly if it is taken into account that this domain does not interact directly with the enzyme. This is supported by the important loss of inhibitory activity of the native forms of ACIshort1 and even more of ACIshort2. On the other hand, the IIIa unfolding intermediate of the whole molecule, displaying the same disulfide bonding as ACIshort1, shows a 20-fold increase in inhibitory capability compared to ACIshort1 against hCPA1. This could imply that the presence of the polypeptide backbone of the NTD is sufficient for an efficient inhibition of the target enzyme without any need of cross-links provided by disulfide bonds. It would also suggest the presence of contacts at the interface between both domains that would be important for the proper positioning of the molecule for a native-like binding to MCPs. In fact, a detailed analysis of the ACI structure reveals several hydrogen bonds and hydrophobic interactions that link both domains (Figure 6). However, this has to be taken cautiously since the structure of free ACI has not been determined yet and some internal contacts could be caused by the binding to the carboxypeptidase and/or the crystalline state of the complex. On the other hand, the deletion of the NTD could alter the acquisition of the native conformation of the CTD, giving rise to a folded form divergent from that of native ACI, with a lower inhibitory capability. In the case of ACIshort2, a 1500-fold affectation on the inhibition constant of the native form compared to native ACI is observed. This dramatic change is probably due to the loss of interactions between the end of the CS (Phe^{39}) and the surface of hCPA1 (see Figure 6 and ref *19*). The presence of a third disulfide bond in ACIshort1 would constrain the conformation of the connecting α-helix, allowing a proper interaction with the enzyme and therefore a stronger complex formation.

The acidic pH strongly minimizes disulfide reshuffling and favors disulfide reduction; therefore the reductive unfolding experiments performed at this pH give information about the disulfide bonds more prompt to reduce. The reductive unfolding of ACI performed at acidic pH shows the accumulation of 4S, 3S and 2S species. Both 4S and 3S species, which are the first to accumulate, lack the disulfide bonds that belong to the NTD, indicating that these disulfides are more solvent accessible than those present in the CTD. As stated above, this would enable the NTD to be important for the attainment of a native global structure by facilitating interdomain disulfide reshuffling. At alkaline pH native ACI reduces its five disulfide bonds in a concerted manner without a significant accumulation of intermediates. This is most likely due to the working pH, which favors the prevalence of disulfide reshuffling over reductive reactions, thus preventing the accumulation of intermediates with native disulfide linkages and leading directly to R. Importantly, ACI displays an extremely high disulfide and conformational stability, resisting up to 100 mM DTT and 4 M GdnHCl, similarly to other

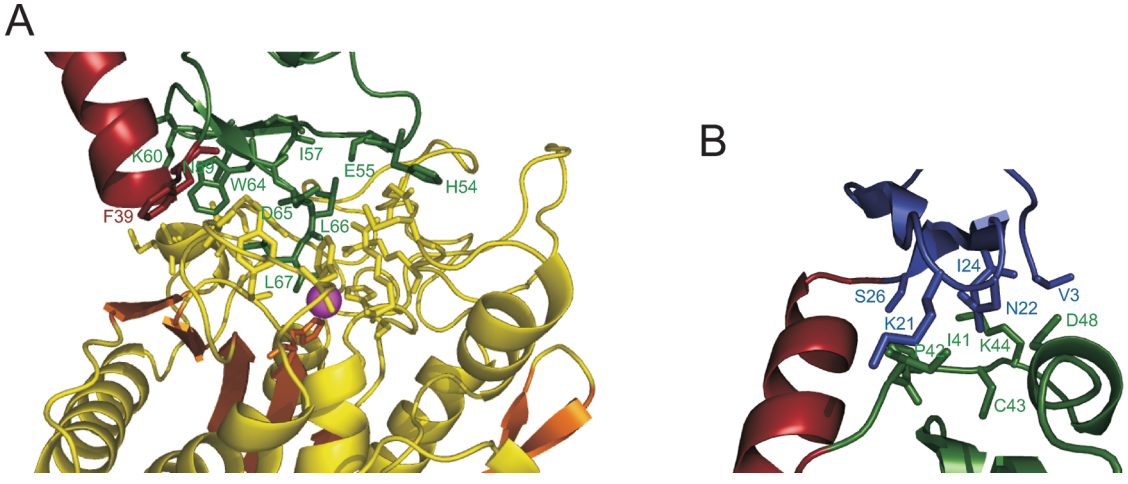

FIGURE 6: Structural details of ACI and its binding with hCPA1. (A) Close-up view of the interface between ACI (CS in red and CTD in green) and hCPA1 (α-helices and turns in yellow, β-strands in orange, catalytic zinc ion as a magenta sphere). The side chains of ACI that interact with the protease are displayed in a stick model and labeled. (B) Close-up view of the interaction between the NTD (in blue) and CTD (in green) of ACI. Hydrogen bonds (2.6−3.4 Å): Asn^{22}−Pro^{42}, Asn^{22}−Asp^{48}. van der Waals interactions (<4 Å): Val^{3}−Lys^{44}, Lys^{21}−Ile^{41}, Asn^{22}−Ile^{41}, Ile^{24}−Cys^{43}, Ser^{26}−Pro^{42}.

compactly folded protease inhibitors such as hirudin or LCI (*32*). This property might be very useful for a molecule designed to act in harsh environments like the intestine of the *Ascaris* hosts or the tissues through which the larvae of this parasite migrate during their life cycle. A high resistance of ACI in front of proteolytic enzymes, together with its strong inhibition of digestive and mast-cell carboxypeptidases, may help to prolong the survival of this parasite inside the host. Overall, the findings derived from the analysis of ACI and its truncated variants constitute a basis for the design of novel variants of minimal size able to target MCPs of potential biotechnological or biomedical interest (*33*).

ACKNOWLEDGMENT

We are indebted to Prof. F. Xavier Gomis-Rüth for helpful suggestions to the manuscript. We also thank the Proteomics and Bioinformatics facility from UAB (Spain), a member of ProteoRed network.

REFERENCES

1. Creighton, T. E. (1986) Disulfide bonds as probes of protein folding pathways. *Methods Enzymol. 131*, 83–106.
2. Creighton, T. E. (1997) Protein folding coupled to disulphide bond formation. *Biol. Chem. 378*, 731–744.
3. Dobson, C. M. (2001) Protein folding and its links with human disease. *Biochem. Soc. Symp.* 1–26.
4. Ross, C. A., and Poirier, M. A. (2004) Protein aggregation and neurodegenerative disease. *Nat. Med. 10* (Suppl.), S10–17.
5. Ventura, S., and Villaverde, A. (2006) Protein quality in bacterial inclusion bodies. *Trends Biotechnol. 24*, 179–185.
6. Chatrenet, B., and Chang, J. Y. (1993) The disulfide folding pathway of hirudin elucidated by stop/go folding experiments. *J. Biol. Chem. 268*, 20988–20996.
7. Darby, N. J., Morin, P. E., Talbo, G., and Creighton, T. E. (1995) Refolding of bovine pancreatic trypsin inhibitor via non-native disulphide intermediates. *J. Mol. Biol. 249*, 463–477.
8. van den Berg, B., Chung, E. W., Robinson, C. V., Mateo, P. L., and Dobson, C. M. (1999) The oxidative refolding of hen lysozyme and its catalysis by protein disulfide isomerase. *EMBO J. 18*, 4794–4803.
9. Welker, E., Narayan, M., Wedemeyer, W. J., and Scheraga, H. A. (2001) Structural determinants of oxidative folding in proteins. *Proc. Natl. Acad. Sci. U.S.A. 98*, 2312–2316.
10. Bulaj, G., and Olivera, B. M. (2008) Folding of conotoxins: formation of the native disulfide bridges during chemical synthesis and biosynthesis of Conus peptides. *Antioxid. Redox Signaling 10*, 141–155.
11. Chang, J. Y., Li, L., and Lai, P. H. (2001) A major kinetic trap for the oxidative folding of human epidermal growth factor. *J. Biol. Chem. 276*, 4845–4852.
12. Cemazar, M., Gruber, C. W., and Craik, D. J. (2008) Oxidative folding of cyclic cystine knot proteins. *Antioxid. Redox Signaling 10*, 103–111.
13. Guo, Z. Y., Qiao, Z. S., and Feng, Y. M. (2008) The in vitro oxidative folding of the insulin superfamily. *Antioxid. Redox Signaling 10*, 127–139.
14. Chang, J. Y. (2008) Diversity of folding pathways and folding models of disulfide proteins. *Antioxid. Redox Signaling 10*, 171–177.
15. Arolas, J. L., Aviles, F. X., Chang, J. Y., and Ventura, S. (2006) Folding of small disulfide-rich proteins: clarifying the puzzle. *Trends Biochem. Sci. 31*, 292–301.
16. Chang, J. Y. (2004) Evidence for the underlying cause of diversity of the disulfide folding pathway. *Biochemistry 43*, 4522–4529.
17. Weissman, J. S., and Kim, P. S. (1991) Reexamination of the folding of BPTI: predominance of native intermediates. *Science 253*, 1386–1393.
18. Chang, J. Y., Schindler, P., and Chatrenet, B. (1995) The disulfide structures of scrambled hirudins. *J. Biol. Chem. 270*, 11992–11997.
19. Sanglas, L., Aviles, F. X., Huber, R., Gomis-Ruth, F. X., and Arolas, J. L. (2009) Mammalian metallopeptidase inhibition at the defense barrier of Ascaris parasite. *Proc. Natl. Acad. Sci. U.S.A. 106*, 1743–1747.
20. Bieth, J. G. (1995) Theoretical and practical aspects of proteinase inhibition kinetics. *Methods Enzymol. 248*, 59–84.
21. Arolas, J. L., Bronsoms, S., Lorenzo, J., Aviles, F. X., Chang, J. Y., and Ventura, S. (2004) Role of kinetic intermediates in the folding of leech carboxypeptidase inhibitor. *J. Biol. Chem. 279*, 37261–37270.
22. Chang, J. Y., Li, L., and Bulychev, A. (2000) The underlying mechanism for the diversity of disulfide folding pathways. *J. Biol. Chem. 275*, 8287–8289.
23. Chang, J. Y. (1997) A two-stage mechanism for the reductive unfolding of disulfide-containing proteins. *J. Biol. Chem. 272*, 69–75.
24. Arolas, J. L., Bronsoms, S., Ventura, S., Aviles, F. X., and Calvete, J. J. (2006) Characterizing the tick carboxypeptidase inhibitor: molecular basis for its two-domain nature. *J. Biol. Chem. 281*, 22906–22916.
25. Weissman, J. S., and Kim, P. S. (1993) Efficient catalysis of disulphide bond rearrangements by protein disulphide isomerase. *Nature 365*, 185–188.
26. Chang, J. Y. (1994) Controlling the speed of hirudin folding. *Biochem. J. 300* (Part 3), 643–650.
27. Pantoja-Uceda, D., Arolas, J. L., Garcia, P., Lopez-Hernandez, E., Padro, D., Aviles, F. X., and Blanco, F. J. (2008) The NMR structure and dynamics of the two-domain tick carboxypeptidase inhibitor reveal flexibility in its free form and stiffness upon binding to human carboxypeptidase B. *Biochemistry 47*, 7066–7078.
28. Arolas, J. L., Pantoja-Uceda, D., Ventura, S., Blanco, F. J., and Aviles, F. X. (2008) The NMR structures of the major intermediates of the two-domain tick carboxypeptidase inhibitor reveal symmetry in its folding and unfolding pathways. *J. Biol. Chem. 283*, 27110–27120.
29. Arolas, J. L., Popowicz, G. M., Lorenzo, J., Sommerhoff, C. P., Huber, R., Aviles, F. X., and Holak, T. A. (2005) The three-dimensional structures of tick carboxypeptidase inhibitor in complex with A/B carboxypeptidases reveal a novel double-headed binding mode. *J. Mol. Biol. 350*, 489–498.
30. Shinde, U., and Inouye, M. (2000) Intramolecular chaperones: polypeptide extensions that modulate protein folding. *Semin. Cell Dev. Biol. 11*, 35–44.
31. Hidaka, Y., Shimono, C., Ohno, M., Okumura, N., Adermann, K., Forssmann, W. G., and Shimonishi, Y. (2000) Dual function of the propeptide of prouroguanylin in the folding of the mature peptide: disulfide-coupled folding and dimerization. *J. Biol. Chem. 275*, 25155–25162.
32. Chang, J. Y., Lin, C. C., Salamanca, S., Pangburn, M. K., and Wetsel, R. A. (2008) Denaturation and unfolding of human anaphylatoxin C3a: an unusually low covalent stability of its native disulfide bonds. *Arch. Biochem. Biophys. 480*, 104–110.
33. Arolas, J. L., Vendrell, J., Aviles, F. X., and Fricker, L. D. (2007) Metallocarboxypeptidases: emerging drug targets in biomedicine. *Curr. Pharm. Des. 13*, 349–366.